Synthesis and catalytic performance of CeOCl in Deacon reaction

Ramzi Farra[a,*], Frank Girgsdies[a], Wiebke Frandsen[a], Maike Hashagen[a], Robert Schlögl[a], Detre Teschner[a]

[a] Fritz-Haber-Institute der Max-Planck-Gesellschaft, Faradayweg 4-6, Berlin, Germany.
E-mail: farra@fhi-berlin.mpg.de,
Fax: +49 30 84134676; Tel: +49 30 84135408

Abstract

Surface chlorinated CeO_2 is an efficient material for HCl oxidation, which raises the question whether an oxychloride phase could be also active in the same reaction. CeOCl was synthesized by solid state reaction of cerium oxide with anhydrous cerium chloride and tested in HCl oxidation using various feed compositions at 703 K. X-ray diffraction of post-reaction samples revealed that CeOCl is unstable, in both oxygen-rich and lean-conditions. Applying oxygen over-stoichiometric feeds led to complete transformation of CeOCl into CeO_2. Considerable HCl conversions were obtained only after this transformation, which confirms the essential role of bulk cerium oxide in this catalytic system.

Graphical abstract

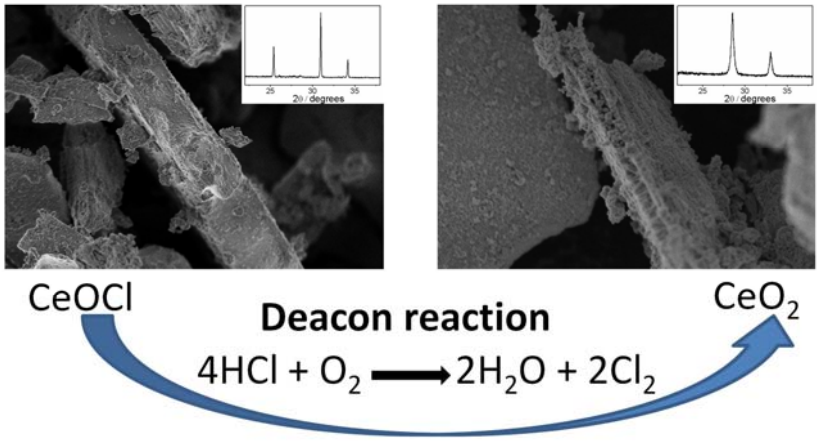

Phase transformation of CeOCl into CeO_2 under Deacon reaction conditions

Keywords: CeOCl, CeO_2, Deacon Reaction, HCl oxidation

1. Introduction

The formation of CeOCl phase under reaction conditions or during sample preparation treatments has been experimentally verified in various heterogeneous catalytic systems[1–4]. In most cases, however, the formation of CeOCl is unintentional. This phase results from the interaction of cerium oxide with chlorine atoms. The origin and function of the components building up the cerium oxychloride differ according to the catalytic system used. For example, CeO_2 is utilized as a carrier in various catalytic systems (i.e. Pd/CeO_2, Rh/CeO_2). In this case Cl atoms may originate from chlorine-containing metal precursors ($RhCl_3$ or $PdCl_2$). Kepinski et al.[5] have studied by means of X-ray diffraction (XRD) and High Resolution Electron Microscopy (HREM) the mechanism of CeOCl formation in Pd/CeO_2 catalyst prepared from $PdCl_2$. They found that Cl atoms adsorbed on the surface of the ceria support are progressively incorporated into the oxygen vacancies as the reduction temperature increased. Ceria can be used also as a bulk catalytic material. In this case, chlorine-containing reactants (HCl or CCl_4) can dissociatively adsorb onto it, and consequently, Cl atoms may incorporate into cerium oxide and forming the CeOCl phase[1, 6, 7].

A comprehensive understanding of ceria-chlorine interaction and the nature of the halogenated oxide surface have drawn more attention recently, due to the newest findings of utilizing CeO_2 as a catalyst for the oxidative halogenation of CH_4[8, 9].

CeO_2 has been identified recently also as an efficient catalyst for HCl oxidation to chlorine (the Deacon reaction)[10] in the temperature range of 623-723 K[11, 12]. Our previous studies have shown that CeO_2 suffers from bulk chlorination and hence deactivation when it is exposed to stoichiometric or sub-stoichiometric Deacon feeds (O_2:HCl ≤ 0.25)[11, 13]. Furthermore, conducting the reaction at relatively low temperatures (<683 K) induces bulk chlorination too, even if over-stoichiometric feeds were applied[13]. The formation of the inactive $CeCl_3 \cdot 6H_2O$ phase was assigned as the

main cause of losing reactivity upon bulk chlorination[11]. However, the quantitative analysis of the chlorine uptake studied by X-ray photoelectron spectroscopy has suggested that even if the catalyst was exposed to O_2-rich feeds (O_2:HCl = 2) at high temperature (703 K) chlorination in the very first subsurface layer could take place. Chlorine atoms can occupy surface sites as well as lattice oxygen vacancies, but yet no structural details are available for this chlorinated surface phase. This raises the question as to whether the bulk CeO_2 material has any influence on the catalytic performance or solely the coexistence of chlorine and oxygen species on the surface is an essential prerequisite for the reactivity of the catalyst. Moreover, using in situ techniques LaOCl was identified as an active intermediate phase catalyzing the destruction of chlorinated hydrocarbons with steam over lanthanide oxide-based catalysts[14]. Thus, similarly CeOCl may be also a candidate for an active surface phase in HCl oxidation. To answer these questions we have synthesized cerium oxychloride to assess its stability and catalytic performance under different Deacon reaction conditions. This phase has chlorine and oxygen species present in bulk and surface, as well, which can facilitate the assessment of the role of the surface O/Cl species and of the bulk CeO_2.

2. Experimental

2.1. Sample preparation

The polycrystalline CeOCl sample was prepared by solid state reaction between cerium oxide (Aldrich, 99%) and anhydrous cerium chloride (Aldrich, 99.9%). Excess amount of chloride was used to force the reaction to completion. A powder mixture of CeO_2 and $CeCl_3$ (molar ratio CeO_2:$CeCl_3$ = 1:2) was pressed into small pellets and placed in a horizontal quartz reactor tube surrounded by an oven. The solid state reaction was carried out in Ar flow (100 cm^{-3} min^{-1}) at 1023 K for 10 hours, then cooled down to room temperature in Ar flow. The pellets retained their form (not melted), and

their yellowish color turned white after reaction. The product was ground and washed using distilled water in order to dissolve the unreacted excess quantity of $CeCl_3$. Thereafter, the precipitate was filtered and dried in air at 353 K for 15 h. The CeOCl (untreated) and CeOCl (after washing and drying treatment) will be referred hereafter as CeOCl-F and CeOCl-T, respectively. To the best of our knowledge, this is first time CeOCl has been intentionally synthesized from cerium chloride and cerium oxide via solid state reaction.

2.2 Characterization methods

XRD data were collected using a Bruker AXS D8 Advance Theta–theta diffractometer in Bragg–Brentano geometry, equipped with a Cu anode, a secondary graphite monochromator ($CuK\alpha_{1+2}$ radiation) and a scintillation counter. Patterns were recorded between 10 and 100° 2θ with a step width of 0.02° and a counting time of 15 s per step. The specific surface area was determined by nitrogen adsorption at 77 K using a Quantachrome 6 port BET system. Prior to the measurements the samples were evacuated for 5 h at 423 K. Thermogravimetric experiments (TGMS) were done on a NETZSCH Jupiter thermobalance in flowing argon (100 cm^3 min^{-1}). The gas evolution was measured with a quadrupole mass spectrometer (Pfeiffer Vacuum, Omnistar). Scanning electron microscopy (SEM) was conducted with a Hitachi S-4800 FEG and the micrographs were taken in the secondary electron (SE) mode at an accelerating voltage of 1.5 kV.

2.3. Catalytic test

The gas phase oxidation of hydrogen chloride was studied at ambient pressure at 703 K. Freshly prepared cerium oxychloride samples were utilized to investigate the catalytic activity of this phase under different O_2 to HCl feed ratios. 0.5g of

polycrystalline CeOCl was loaded in the tubular reactor (8 mm i.d.) and pretreated in N_2 at 703 K for 30 min. Thereafter, the reaction gases were introduced at a total flow of 166 cm^3 min^{-1}. Various feed compositions were tested, which can be sorted out into two categories according to the oxygen partial pressure used: oxygen-rich (O_2:HCl = 9 and 4) and oxygen-lean conditions (O_2:HCl = 0.5 and 0.25). 5 h tests were carried out with fresh loads of CeOCl-T for each O_2:HCl ratio. Post-reaction samples were collected for BET, SEM and XRD characterizations after rapidly cooling down the reactor to room temperature in a flow of N_2. Reactivity was followed by means of iodometric titration.

3. Results and discussion

3.1. Synthesis and stability of CeOCl

Several synthesis routes to prepare rare-earth oxychlorides are known based on different ways to introduce the chlorine atom in the structure. Ammonium chloride has been used most frequently as chlorinating agent[15–18]. The solid state reaction of rare-earth oxide with NH_4Cl is taking place at temperatures (973-1273 K)[17] much higher than the ammonium chloride's sublimation temperature (611 K). Therefore, excess amount of NH_4Cl must be used at controlled temperature and flow. First, we have taken this approach for the synthesis of CeOCl. The primary results obtained from a thermal gravimetric analysis (TGA) experiments were promising in terms of phase purity, but our attempts failed in scaling up this procedure.

Depner et al.[19] have developed a new route to synthesis CeOCl nanocrystals based on the condensation of cerium alkoxides with cerium halides. Depending on the alkoxide and halide precursors used it is possible to tune the composition and the size of the obtained nanocrystals. LaOCl was synthesized by mechano-chemical grinding of the corresponding oxide and chloride compounds[20].

Our CeOCl sample was prepared by solid state reaction of cerium oxide with excess amount of anhydrous cerium chloride, as detailed in the Experimental section. The XRD patterns of CeOCl-T, CeOCl-F samples are shown in Figure1 (a and b respectively) and compared to the pattern of CeOCl reference[21]. The diffractograms confirm the solid state reaction, and CeO_2 reflections are not obviously visible in either sample. However, fitting of the CeOCl-T diffractogram suggests 3 % minority CeO_2 phase still present in the final material. The major impurity, as additional peaks with minor intensity, in the untreated sample (CeOCl-F) can be assigned to $CeCl_3 \cdot 7H_2O$ from the unreacted excess of $CeCl_3$ precursor. This was washed out by water to obtain the final material. CeOCl has a PbFCL type crystal structure (tetragonal space group *P*4/*nmm*) with *a* = 4.08, *c* = 6.83 Å [20]. In this structure, the cerium has a 9-fold (capped square anti-prismatic) coordination environment, with four oxygen atoms forming the smaller basal square and 4+1 chlorine atoms a larger, mono-capped square plane.

Furthermore, the relative intensities of the CeOCl-T reflections indicate a pronounced preferred orientation, while this effect is only weakly developed in the sample before treatment. This indicates that a re-crystallization process took place during the cleaning process, producing more anisotropic crystallite morphology. The SEM photographs (Fig. 2a) of CeOCl-T confirm this observation and clearly display a plate-like morphology of the CeOCl-T particles with an average thickness of 2-3 µm and a particle size ranging from 5 to 20 µm. The BET surface area of CeOCl is relatively low (8.7 m^2g^{-1}). The stability of CeOCl has been tested by means of thermogravimetric analysis coupled to mass spectroscopy (TGA-MS). The sample was heated up to 973 K (2 K min^{-1}) in Ar flow (100 cm^3 min^{-1}). The TGA curve (Fig. 3a) shows that the sample is essentially stable over the whole temperature range studied, and the minor weight loss of 0.5% at 573 K could be assigned according to the corresponding MS signal to the desorption of water molecules. Aging effect has been studied, in which the CeOCl-T sample was left exposed to ambient atmosphere over a long period of time (5

months), and thereafter its XRD spectrum was measured again. Over time water molecules adsorbed on the surface interact with CeOCl giving rise to phase transformation partially into $Ce(OH)_2Cl$ (Fig. 4a). However, the original CeOCl phase can easily be restored by heating the sample in inert gas (Ar) (Fig. 4a), in which the evolution of water is observed at 570 K (Fig. 3b). No further decomposition was found at higher temperatures.

3.2. Catalytic activity of CeOCl in HCl oxidation

Freshly prepared CeOCl samples were tested as Deacon catalyst by exposing them to reaction feeds with different O_2:HCl ratios at 703 K (Fig. 5a). The used samples were analyzed afterwards by XRD (Fig. 4b). In O_2-lean regime (O_2:HCl = 0.25 or 0.5) HCl conversion was very low (< 3%). The lowest O_2:HCl = 0.25 ratio led to the complete deactivation of the catalyst over time, whereas at O_2:HCl = 0.5 a very slight increase in reactivity trend was observed.

Beside CeOCl, CeO_2, $CeCl_3 \cdot 3H_2O$ and $CeCl_3 \cdot 6H_2O$ were observed in the used sample exposed to the lowest feed ratio O_2:HCl = 0.25, CeO_2 being a significant component. CeO_2 was the dominant phase in the case of O_2:HCl = 0.5. These results reveal that chlorination and de-chlorination are competing processes under these conditions, and furthermore the phase transformation to chloride is more likely passing through the formation of the corresponding oxide first.

Samples exposed to relatively high feed ratio, O_2:HCl = 2 and 9, have shown that the original CeOCl was fully transformed into CeO_2 (Fig. 4b). At O_2:HCl = 2, the initially low HCl conversion progressively increased, reaching the activity level exhibited by a pure reference ceria at identical conditions[11]. Furthermore, $CeCl_3 \cdot 6H_2O$ transformed also to CeO_2 under these conditions reaching similar reactivity[13]. The highest HCl conversion (~37%) was achieved by using excess of O_2 at feed ratio O_2:HCl = 9. An overshooting

of HCl conversion observed at the beginning of the reaction can be plausibly assigned to the additional contribution of Cl_2 produced during the transformation of CeOCl to CeO_2 and the high exothermicity of this transformation. This process depends on the $p(O_2)$ used in the feed, and hence is faster for CeOCl sample exposed to higher O_2:HCl ratio. The SEM photograph (Fig. 2c) of the used sample (O_2:HCl = 9) shows that the plate-like morphology is retained but the particles themselves consist of compact agglomeration of very fine particles (Fig. 2d). This is in line with the surface area increase of the samples after reaction (BET = 28 m^2/g for O_2:HCl = 9). The average Cl_2 productivity of CeOCl samples measured at different O_2:HCl feed ratios (O_2:HCl = 0.25, 0.5, 2 and 9) is plotted in Fig. 5b. It is known that the apparent O_2 reaction order of pure CeO_2 is ~0.5[11]. Since XRD suggested the formation of CeO_2, a theoretical 0.5 order curve representative of CeO_2 is also included in Fig. 5b, and is aligned at O_2:HCl = 2 with the measured dataset. Not surprisingly, the data point at O_2:HCl = 9 follows reasonably the trend. However, the oxygen lean points are clearly inferior. This discrepancy can be partially rationalized considering that the surface area of the CeO_2 is larger than that of CeOCl, and the partially formed chloride phase is inactive in Deacon conditions.

Since CeOCl is not stable in either O_2-rich or lean conditions, its intrinsic catalytic performance could not be assessed. Nevertheless, the results suggest that the sole existence of surface O and Cl species in the oxychloride matrix is not enough to maintain stable HCl oxidation reactivity and the existence of the bulk cerium oxide phase seems to be a prerequisite to ensure efficient and stable catalytic performance. The bulk oxide structure offers oxygen vacancies that are required for the O_2 activation process. Furthermore, its surface can withstand high degree of chlorination without phase transformation into chloride if oxygen over-stoichiometry is maintained. In spite of the catalytic reaction taking place on the surface, the co-existence of a slightly

oxygen deficient bulk phase (CeO_2 with O vacancies) facilitating the mobility of vacancies between bulk and surface seems to be indispensable in this system.

4. Conclusion

Cerium oxide is now a well-established HCl oxidation catalyst with a high degree of surface chlorination. Since HCl oxidation requires both HCl and O_2 activation, both reactants need to coexist on the catalyst surface. Here, we synthesized and tested CeOCl in HCl oxidation in order to assess the importance of bulk oxide phase in the ceria system and to find out whether the sole presence of surface O and Cl species incorporated into the catalyst surface is enough to achieve stable and efficient catalytic performance. Our experiments have shown that CeOCl is not stable in HCl oxidation, neither in oxygen-lean nor in oxygen-rich conditions. The results suggest that the bulk oxide phase plays a significant role in the cerium oxide based HCl oxidation system, probably facilitating efficient O_2 activation via bulk and surface O-vacancy dynamics with the ability to dissociatively adsorb HCl, without giving rise to phase transition in an oxygen over-stoichiometric reaction feed.

References

1. Weckhuysen BM, Rosynek MP, Lunsford JH (1999) Phys Chem Chem Phys 1:3157–3162.

2. Fajardie F, Tempere O, Manoli J-M, Djega-Mariadassou G, Blanchard G (1998) J Chem Soc, Faraday Trans 94:3727–3735.

3. Kepiński L, Wołcyrz M, Okal J (1995) J Chem Soc, Faraday Trans 91:507–515.

4. Le Normand F, Barrault J, Breault R, Hilaire L, Kiennemann A (1991) J Phys Chem 95:257–269.

5. Kepinski L, Okal J (2000) J Catal 192:48–53.

6. De Rivas B, Lopez-Fonseca R, Gutierrez-Ortiz MA, Gutierrez-Ortiz JI (2011) Appl Catal B-Environ 104:373–381.

7. Farra R, Wrabetz S, Schuster ME, Stotz E, Hamilton NG, Amrute AP, Pérez-Ramírez J, López N, Teschner D (2013) Phys Chem Chem Phys 15:3454–3465.

8. He J, Xu T, Wang Z, Zhang Q, Deng W, Wang Y (2012) Angew Chem-Int Edit 51:2438–2442.

9. Hu Z, Metiu H (2012) J Phys Chem C 116:6664–6671.

10. Perez-Ramirez J, Mondelli C, Schmidt T, Schlüter OF-K, Wolf A, Mleczko L, Dreier T (2011) Energy Environ Sci 4:4786–4799.

11. Amrute AP, Mondelli C, Moser M, Novell-Leruth G, López N, Rosenthal D, Farra R, Schuster ME, Teschner D, Schmidt T, Pérez-Ramírez J (2012) J Catal 286:287–297.

12. Moser M, Mondelli C, Schmidt T, Girgsdies F, Schuster ME, Farra R, Szentmiklósi L, Teschner D, Pérez-Ramírez J (2013) Appl Catal B-Environ 132:123–131.

13. Farra R, Eichelbaum M, Schlögl R, Szentmiklósi L, Schmidt T, Amrute AP, Mondelli C, Pérez-Ramírez J, Teschner D (2013) J Catal 297:119–127.

14. Weckhuysen BM (2003) Phys Chem Chem Phys 5:4351–4360.

15. Hölsä J, Niinistö L (1980) Thermochimica Acta 37:155–160.

16. Song K, Kauzlarich SM (1994) Chem Mater 6:386–394.

17. Hölsä J, Lahtinen M, Lastusaari M, Valkonen J, Viljanen J (2002) J Solid State Chem 165:48–55.

18. Zhu GC, Li FP, Xiao MG (2003) Trans Nonferrous Met Soc China 13:1454–1458.

19. Depner SW, Kort KR, Jaye C, Fischer DA, Banerjee S (2009) J Phys Chem C 113:14126–14134.

20. Lee J, Zhang Q, Saito F (2001) J Solid State Chem 160:469–473.

21. Wołcyrz M, Kepinski L (1992) J Solid State Chem 99:409–413.

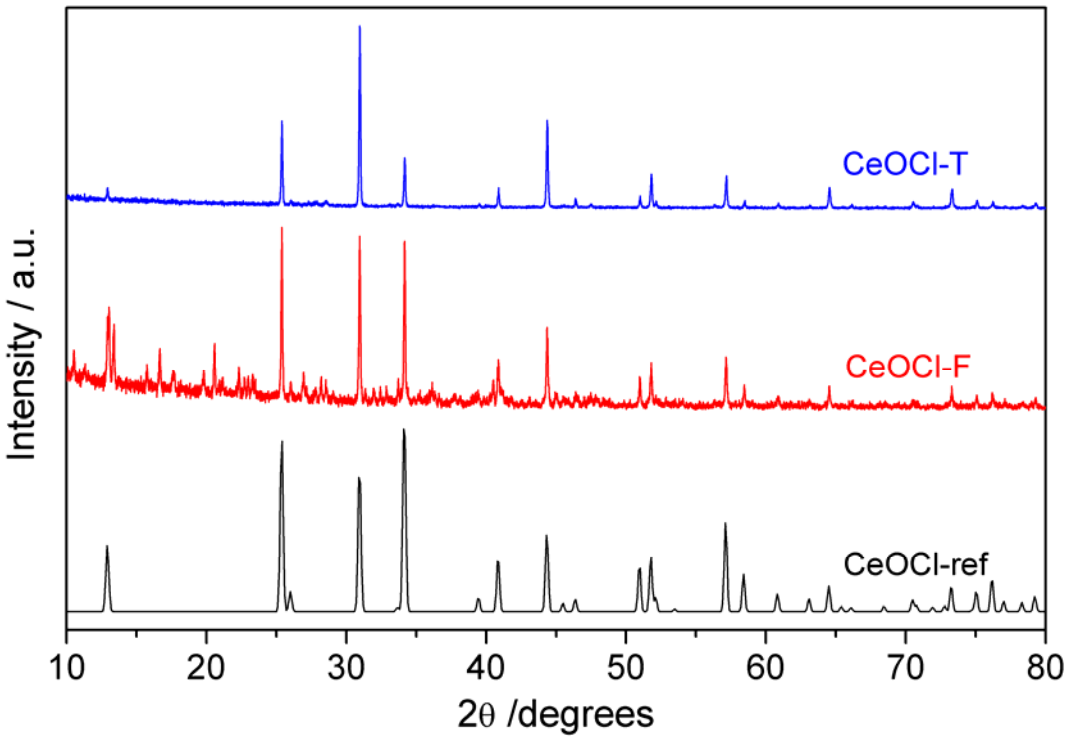

Fig. 1 XRD pattern of CeOCl materials. CeOCl-T after cleaning treatment; CeOCl-F before cleaning treatment and CeOCl-ref as a reference[21].

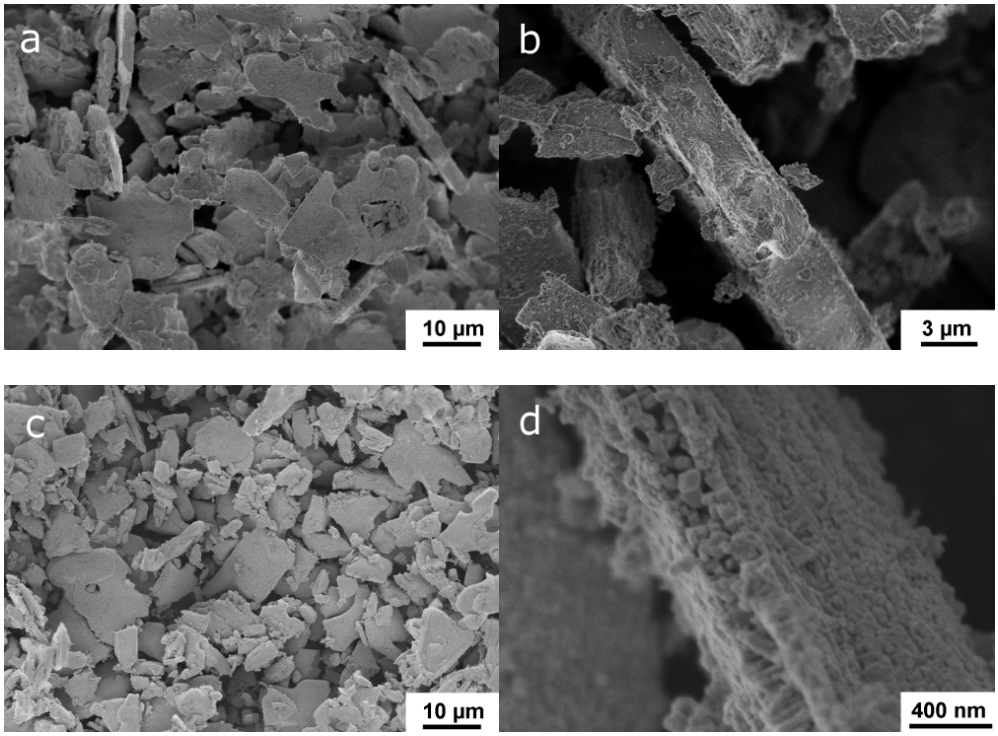

Fig. 2 SEM photographs of CeOCl-T. **a** and **b**: before HCl oxidation, **c** and **d**: after reaction (O_2:HCl = 1:9 at 703 K).

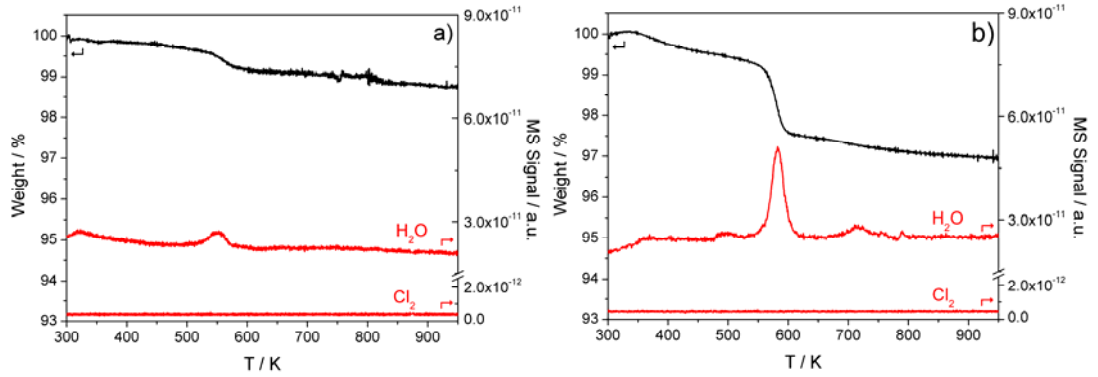

Fig. 3 TGA-MS of CeOCl-T in Ar flow. **a)** fresh material; **b)** after 5 months exposure to ambient air.

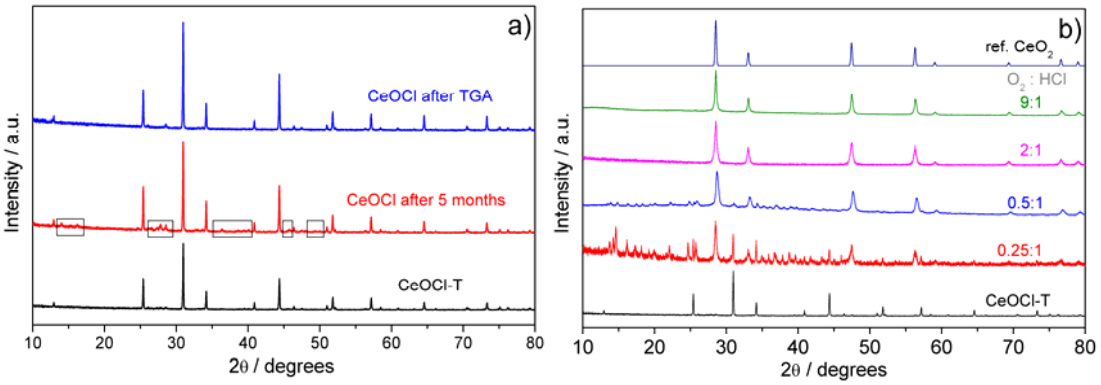

Fig. 4 a) X-ray powder diffraction patterns of CeOCl-T: after 5 months exposure to ambient air (reflections within boxes belong to $Ce(OH)_2Cl$), after TGA treatment of CeOCl-T exposed to air for 5 month with the fresh CeOCl for comparison. **b)** XRD spectra of CeOCl-T samples before and after reaction using different feed ratios, with added CeO_2 reference.

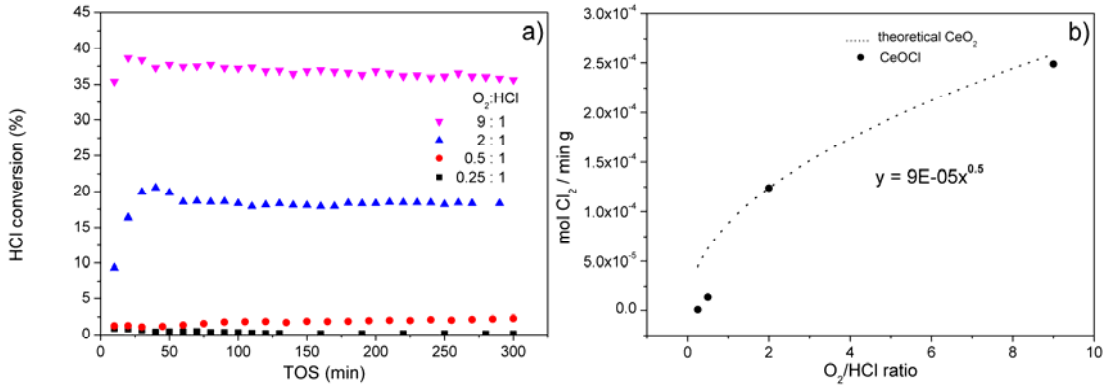

Fig. 5 a) reactivity of CeOCl-T at different feed ratios with time on stream. **b)** comparison of Cl_2 productivity of CeOCl at different O_2:HCl ratios with a theoretical 0.5 order dependence observed for CeO_2.